1995 2

3

Improving Milling Performance with High Pressure Waterjet Assisted Cooling / Lubrication

R. Kovacevic
Member ASME

C. Cherukuthota

R. Mohan
Student Member ASME

Center for Robotics
and Manufacturing Systems and
Department of Mechanical Engineering,
University of Kentucky,
Lexington, KY 40506

During machining, due to relative motion between tool and workpiece, severe thermal/frictional conditions exist at the tool-chip interface. Metal machining processes can be more efficient in terms of increasing the metal removal rate and lengthening tool life, if the thermal/frictional conditions are controlled effectively. A high pressure waterjet assisted coolant/lubricant system that can be used in conjunction with rotary tools (e.g., face milling) is developed here. The performance of this system is evaluated in terms of cutting force, surface quality, tool wear, and chip shape. The improvement in the effectiveness of the developed system with increase in water pressure and orifice diameter is also investigated. Stochastic modeling of the surface profile is performed to obtain more information about the role of waterjet in the machining process.

1 Introduction

In the process of machining, a tool penetrates into the workpiece and removes material in the form of chips. A major portion of the energy is consumed in the formation and removal of chips. The greater the energy consumption, the greater are the temperatures and the frictional forces at the tool-chip interface and consequently the higher is the tool wear. Metal machining processes can be more efficient (in terms of lengthening tool life and improving surface finish) if the thermal/frictional conditions at the tool-chip interface are controlled. Removal of heat from the machining system is a natural way to keep the rate of wear under control. Cutting fluids have been traditionally used at the cutting zone for the purpose of heat removal and lubrication. The cooling action of the cutting fluid consists in abstracting the heat generated during the process of cutting, while the lubricating action of the cutting fluid consists of reducing the friction between the tool rake face and the chip. Rate of flow and direction of application of the cutting fluid determine the effectiveness of the cooling/lubrication. A flood of fluid directed over the back side of the chip is the most common way of applying the coolant/lubricant into the cutting zone. In this case, heat generated during the contact of the tool with workpiece is extracted via the chip. However, at higher cutting speeds, it has been proved that the cutting fluids lose their effectiveness as a coolant. This can be attributed to the greater rate of heat generation, the inability of the cutting fluid to reach the regions to be cooled and the tendency of the faster moving chips to carry the cutting fluid away from the cutting zone.

A number of attempts have been made in order to improve cooling in high speed machining and in the case of machining difficult-to-machine materials like titanium. The use of pressurized jet to improve cooling started in 1952 when Pigott and Colwell [1] conducted experiments on a lathe equipped with an oiljet. The oiljet was injected at pressures of 2.75 MPa through a remote nozzle. As a result of this, tool life increased 7 to 8 times, surface quality improved drastically, built-up-edge was eliminated. Ramaiyengar et al. [2] conducted experiments on turning with the help of an internally cooled tool. Cutting forces were reduced by about 60 percent and chip shape improved. Sharma et al. [3] conducted orthogonal machining on a lathe with the cutting fluid being forced directly into the tool-chip interface through a hole in the rake face of the tool. The cutting fluid was injected in the form of a jet of diameter 0.25 mm and a pressure of 68.8 MPa. There was a considerable reduction in the coefficient of friction, consequent decrease in chip curl diameter and improvement in tool life. Mazurkiewicz et al. [4] carried out tests on a screw cutting lathe by injecting waterjet at pressures up to 280 MPa through a remote nozzle. The feed force was reduced drastically (almost 50 percent), coefficient of friction decreased, surface finish improved and metal removal rate increased. A similar idea of high pressure waterjet cooling in turning operation was adopted by Lindeke et al. [5]. However, in this case waterjet, pressurized up to 275 MPa was forced through a hole of 0.125 mm diameter in the carbide insert very close to the cutting edge. They reported that tool life, when cutting titanium alloy, was increased by approximately 500 percent compared to traditional flood cooling.

From all these investigations, it is evident that injecting the cutting fluid at a high pressure into the cutting zone is much more beneficial than the conventional cooling techniques. Also, it was found that attempts made at applying cutting fluid through the rake face of the tool [2, 3, 5, 6] were

Contributed by the Production Engineering Division for publication in the JOURNAL OF ENGINEERING FOR INDUSTRY. Manuscript received Oct. 1993; revised June 1994. Associate Technical Editor: K. Rajurkar.

more beneficial than those [1, 4] in which the cutting fluid was injected through a remote nozzle. A high pressure waterjet brought as a coolant/lubricant through a hole in the rake face of the tool reduces secondary shear, lowers interface temperatures as well as the temperature of the body of the insert, and changes the chip shape. All the attempts made until now are restricted to stationary single edge cutting tool operations like turning. However, there is an urgent need to incorporate the high pressure waterjet cooling technique for rotary tool operations (like milling, drilling, etc.) to increase the metal removal rate, improve the dimensional accuracy and lengthen tool life.

The objective of this work is to develop a coolant/lubricant system for rotary tool operations (e.g., face milling) that will be based on a high pressurized waterjet (up to 380 MPa). The performance of the developed high pressure waterjet cooling technique is evaluated in terms of components of cutting force, surface finish, chip shape and tool life. The face milling cutter used here is equipped with a single insert, having an EDM drilled hole. As the location of the hole on the insert is a crucial factor in determining the effectiveness of the coolant/lubricant system, an on-line optical sensing technique is developed to determine the optimum location of hole in the insert. Also, the performance of the system with variations in water pressures and orifice diameters is evaluated. Workpiece material used for the investigation is stainless steel AISI 304.

2 Experimental Setup and Procedure

A high pressure waterjet coolant/lubricant system has been developed [7] which can be used in conjunction with a vertical milling machine, mounted with a cutter capable of holding five inserts. However, this developed system can be extended for use with any rotary tool operation. A schematic of the designed system is shown in Fig. 1. The developed high pressure coolant/lubricant system uses a high pressure intensifier pump capable of supplying the cutting fluid at pressures up to 380 MPa. The pressurized cutting fluid from the intensifier pump is directed to the main flow channel in the cutter through a rotary swivel, which provides sealing up to a rotational speed of 2000 rpm and pressures up to 380 MPa. The main flow channel extends axially through the cutter and directs the cutting fluid through a plurality of radially extending feed channels. The number of radially extending feed channels is equal to the number of inserts mounted on the cutter. A sapphire orifice is placed at the terminal end of each radially extending feed channel directly behind the cutting insert. Each nozzle provides a stream of cutting fluid travelling at over 300 m/sec which is directed through the EDM drilled hole in the insert. One of the most important factors which determine the effectiveness of high pressure waterjet cooling is the proper location of hole in the insert. Different hole locations were tried and the hole centered at about 1.25 mm from tool tip was found to be an optimum location giving good results without significantly reducing the strength of the tool. Photograph in Fig. 2(*a*) shows the hole corresponding to this location while Fig. 2(*b*) shows the orientation of the jet towards the tool-chip interface. It can be seen from Fig. 2(*b*) that the orientation of the jet is in such a way that it hits the underside of the chip as it is being formed so as to dissipate heat quickly from the hot zones of tool-chip interface.

The experimental setup consists of a vertical milling machine, cutter, high pressure intensifier pump, tubing with rotary swivel, a four component dynamometer, charge amplifiers, A/D converter and PC/AT with suitable software. The workpiece is mounted on the four component dynamometer in order to measure the X, Y, and Z components of the cutting force. A sampling frequency of 2 KHz was selected to acquire the cutting force components. The quality of the machined surface was quantified in terms of roughness average, R_a. The experiments were conducted in two phases. In phase 1, the hydraulic parameters (water pressure and orifice diameter) were kept constant and conventional parameters (cutting speed, feed, depth of cut) were varied at four different levels. In phase 2, the conventional parameters were kept constant (at their nominal values) and experiments were performed by varying water pressure and orifice diameter. The process parameters used in these phases are shown in

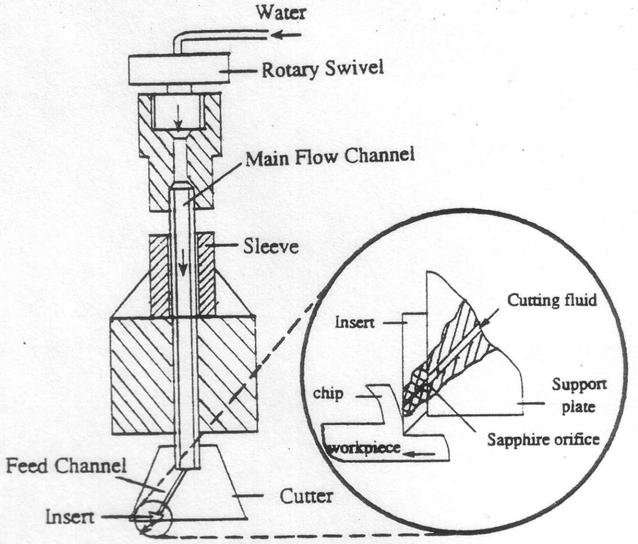

Fig. 1 Design of high pressure waterjet coolant / lubricant system

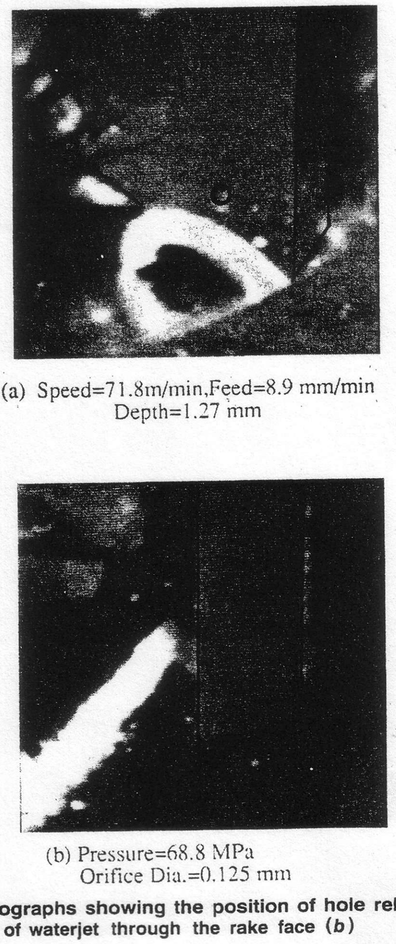

Fig. 2 Photographs showing the position of hole relative to chip (*a*) and flow of waterjet through the rake face (*b*)

Table 1 Process parameters

Constant Conditions		
Workpiece material	-	Stainless Steel AISI 304
Diameter of the Cutter	-	50.8 mm
Type of Operation	-	Face Milling
Max number of Inserts	-	5
Number of Inserts Used	-	1
Type of the Insert Used	-	TPG322 (K313)
Geometry of the Insert	-	Rake Angle=0°
		Nose radius=0.8 mm
		Clearance angle=11°
Experimental Variables - Phase 1		
Range of Cutting Speed	-	47.9 m/min to 95.8 m/min
Range of Cutting Feed	-	5.10 to 12.70 mm/min
Range of Depth of Cut	-	0.51 mm to 1.27 mm
Length of the Cut	-	75 mm
Type of Cooling Used	-	Flood & High Pressure Waterjet
Water Pressure	-	68.8 MPa
Orifice Diameter	-	0.250 mm
Experimental Variables - Phase 2		
Cutting Speed	-	71.8 m/min
Cutting Feed	-	8.9 mm/min
Depth of Cut	-	0.89 mm
Length of the Cut	-	75 mm
Type of Cooling Used	-	Flood & High Pressure Waterjet
Range of Water Pressure	-	0 to 110 MPa
Range of Orifice Diameter	-	0 to 0.45 mm

Table 1. The cutting force components along X, Y and Z directions were monitored in all the cases. The surface roughness was measured and chips produced were collected for analysis. The surface profile data generated by flood cooling and with the assistance of high pressure waterjet cooling is characterized using the stochastic modeling technique of auto regressive moving average (ARMA) modeling to get more information about the role of waterjet in the milling process.

3 Results and Discussion

3.1 High Pressure Waterjet Cooling vs Flood Cooling—Comparison. The experiments in phase 1 were conducted in an attempt to evaluate the effectiveness of high pressure waterjet cooling (applied at a pressure of 68.8 MPa through an orifice of dia. 0.25 mm) as compared to flood cooling. The experiments were conducted over a range of cutting speeds (47–96 m/min), feeds (5–13 mm/min), and depth of cut (0.5–1.3 mm). A new insert was used for every set of experiments performed. Cutting force components, surface quality and chip shapes were analyzed for comparison.

3.1.1 Cutting Force. The cutting force components (average) with change in cutting speed are plotted in Fig. 3(*a*) for flood cooling and high pressure waterjet cooling. It can be noted that all the cutting force components, X, Y and Z are always lower with the application of the high pressure waterjet than in the case of flood cooling. A difference of almost 60 N in the magnitude of the cutting force component in the X direction is maintained between the two types of cooling. The cutting force component in the Y direction increases steeply with increase in the cutting speed. A constant difference of 70 N is observed in the Y component forces. The difference in the Z component of the cutting force for both cooling techniques was initially around 15 N but steadily increased with the cutting speed. The cutting force components (average) with change in feed are plotted in Fig. 3(*b*). The cutting force components obtained with high pressure waterjet cooling are found to be lower than those obtained with flood cooling. The X component under high pressure cooling does not increase as steeply as in the case of flood cooling. The trend in the case of Y component is almost a replica of the pattern obtained in the case of X component signal. The application of the high pressure waterjet is accompanied by a constant reduction of about 33 percent in the Y component force as compared to flood cooling. The difference in the Z component force is maintained steadily at 15 N with a notable difference of about 35 N at higher feed rates. This indicates that the influence of high pressure waterjet is much more pronounced at higher feed rates than in the case of lower feed rates. The influence of depth of cut on the cutting force components for the two different cooling conditions is shown in Fig. 3(*c*). Here also, it is seen that the cutting force components with the application of the high pressure waterjet are much lower than that of flood cooling. The influence of high pressure waterjet is more pronounced at lower depth of cut than at higher depth of cut.

The placement of the high pressure waterjet at the tool-chip interface aids in reducing the tool-chip contact area at the rake face. As a result, the frictional forces at the cutting zone (secondary shear zone) are reduced. This phenomenon can be expected to be responsible for the reduction in the cutting force components along X, Y, and Z directions.

3.1.2 Surface Finish. Typical plots of surface profile signatures obtained in the case of flood cooling and high pressure waterjet cooling are shown in Fig. 4. The change in the surface roughness, R_a with a change in the cutting parameters are plotted in Fig. 5. With increase in the cutting speed, it can be seen that the value of R_a gradually reduces. With an increase in feed, the surface finish deteriorates. The change in the depth of cut does not have a monotonically increasing or decreasing influence on the surface finish. The influence of the high pressure waterjet is more pronounced at lower depths of cut. In all these cases we find that the high pressure waterjet is able to give us a better surface finish compared to that obtained with flood cooling.

As can be seen later, the rate of wear of the tool is less in the case of high pressure waterjet cooling as compared to flood cooling. This is the main cause for obtaining better surface finish with high pressure waterjet cooling.

3.1.3 Chip Shape. Figure 6 shows the typical chip shapes obtained with flood cooling and high pressure waterjet cooling. The chips produced in the case of flood cooling are bigger in size than those produced in the case of high pressure waterjet cooling. It was found that the chips produced during the flood cooling are blackened due to the extreme heat generated at the tool-chip interface. Whereas, the chips produced during the high pressure waterjet cooling have a bright surface indicating that the chips are not burnt. This shows that the thermal/frictional conditions existing at the tool-chip interface in high pressure waterjet cooling are not as severe as in the case of flood cooling.

3.2 Influence of Hydraulic Parameters on the Effectiveness of High Pressure Waterjet Cooling. The experiments in phase 2 were conducted in order to study the effect of varying water pressures (0–110 MPa) and orifice diameters (0–0.45 mm) on the performance of high pressure waterjet cooling. The conventional parameters are kept constant at their nominal values (speed-79.8m/min, feed-8.9 mm/min, depth of cut-0.89 mm). The evaluation of the effectiveness of high pressure cooling is based on the study of cutting force, surface quality, scanning electron microscope (SEM) photographs of the chip, and tool wear.

3.2.1 Cutting Force. A plot of the cutting force components (average) along X, Y, and Z directions against the

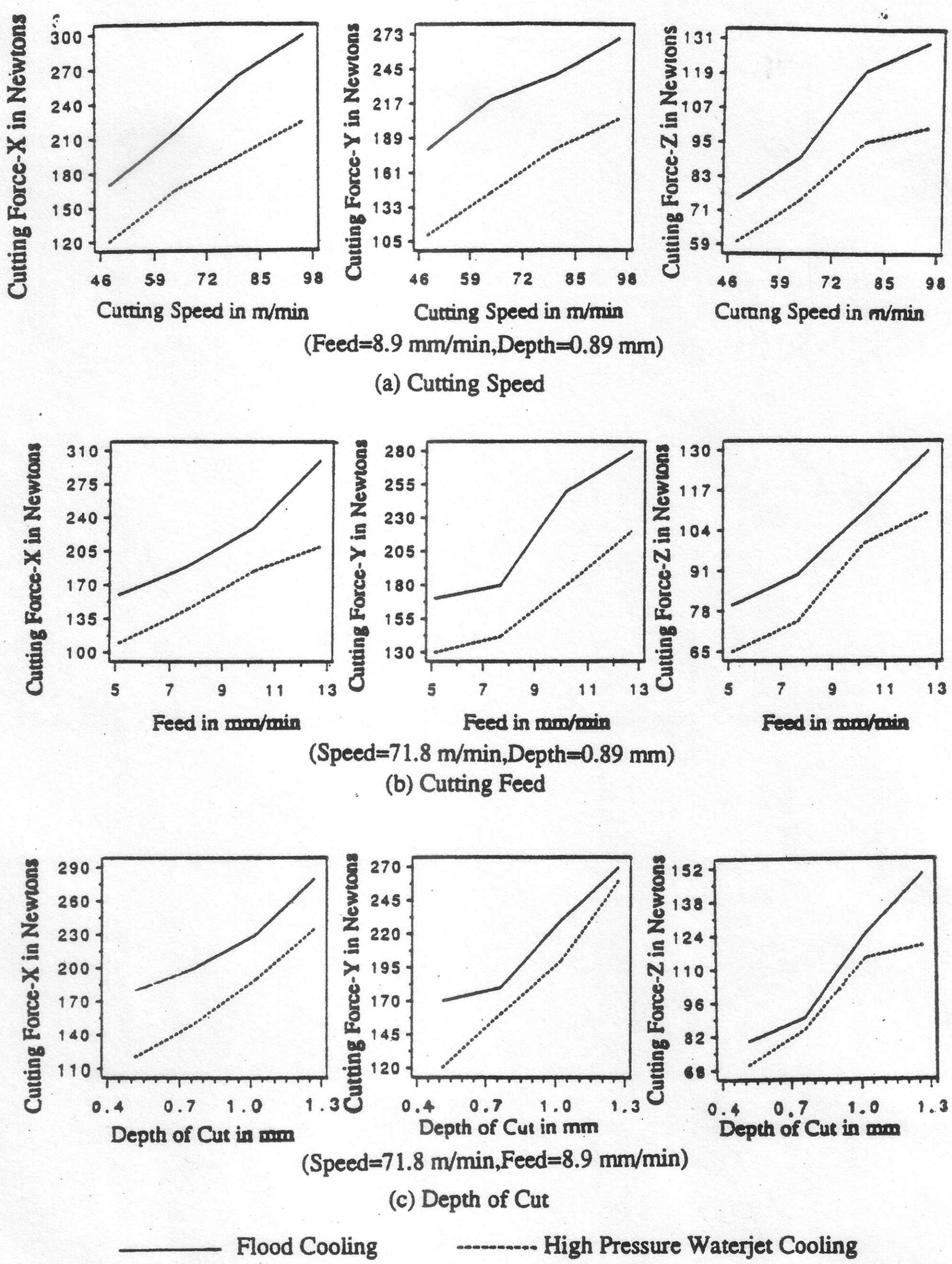

Fig. 3 Components of cutting force vs. (*a*) cutting speed, (*b*) feed and (*c*) depth of cut

variation in water pressure is shown in Fig. 7(*a*). The pressure corresponding to zero indicates flood cooling. The X component of the force is found to reduce steeply with increase in water pressure. The rate of decrease is almost uniform for the entire range of pressure from 0 to 110 MPa. The variation in the cutting force components with increase in the orifice diameters is shown in Fig. 7(*b*). Here also, the X component force reduces with increase in the orifice diameter. Initially, the rate of reduction is very high, but remains steady in the higher range of water pressures and orifice diameters used. This is an indication that after a certain optimum value, a further increase in the volume or pressure of water is not very beneficial to the machining process, considering the additional expenditure incurred in increasing the level of hydraulic parameters. The Y component shows a trend similar to that observed in the case of X component with variation in the pressure and orifice diameter. The Z component reduces steadily with increase in the water pressure. There is a drastic reduction in the Z component with increase in the orifice diameter. However, at larger orifice diameters, the rate of decrease is comparatively less, with the curve approaching the horizontal axis asymptotically.

In the case of high pressure waterjet injected into tool-chip interface through a remote nozzle in turning operation, Mazurkiewicz et al. [4] reported that the formation of hydro-wedge at the tool-chip interface might be the cause for reduction in cutting forces. In the current investigation of high pressure waterjet assisted milling, where the waterjet is injected through the rake face of the tool, the hydraulic wedge between tool and chip could be formed by the jet lateral flow after impingement on chip bottom surface. The above trend in the reduction of the cutting force components with increase in water pressure and orifice diameter shows a strong support for the reasoning in the formation of hydraulic wedge. The increase in water pressure or orifice diameter leads to a steady growth in the wedge formation. This hydro-wedge gradually reduces the area of contact between the chip and rake face consequently decreasing the friction at the tool-chip interface, which attributes to reduction of the cutting force. The reduction in the coefficient of friction at the tool/chip interface with the application of high pressure waterjet can reduce conditions from seizure to sliding even under severe machining conditions [4].

3.2.2 Surface Finish. The variation in the value of the roughness average, R_a, with change in the water pressure and orifice diameter is shown in Fig. 8(a) and Fig. 8(b) respectively. The R_a corresponding to zero water pressure and zero orifice diameter represent flood cooling. It can be clearly seen that increase in water pressure and orifice diameter will improve the surface finish. The quality of the surface obtained depends to a great extent on the tool wear. With increase in water pressure and/or the orifice diameter, the rate of tool wear reduces, increasing the tool life which leads to a better surface finish.

3.2.3 Surface Profile Characterization. The dynamic characteristics of the surface obtained by high pressure waterjet cooling are derived using stochastic modeling technique in order to understand more about the role played by the hydraulic parameters in the process of surface generation. Let the surface profile obtained be described by the following ARMA(n,n-1) model,

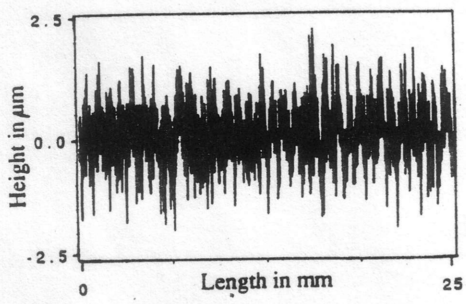

(a) Flood Cooling

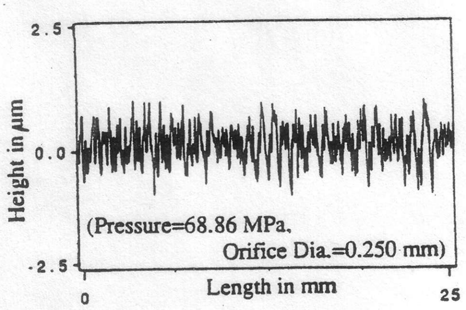

(b) High Pressure Waterjet Cooling

(Speed=71.8 m/min, Feed=8.9 mm/min, Depth=0.89 mm)

Fig. 4 Typical surface profile signatures

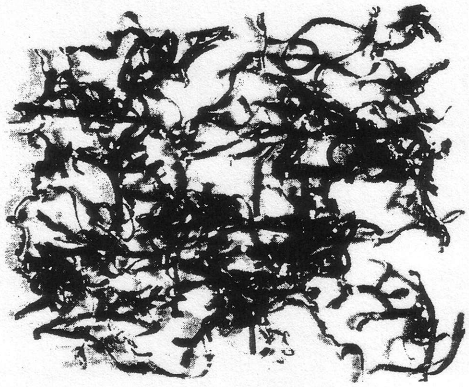

(a) Flood Cooling

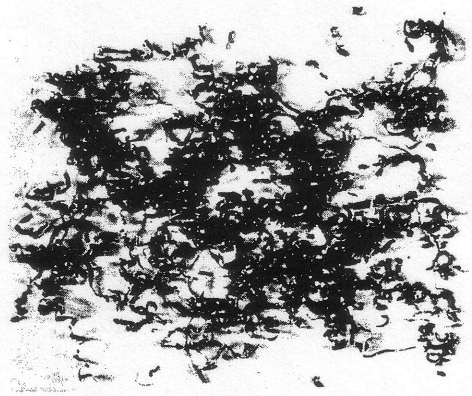

(b) High Pressure Waterjet Cooling

(Pressure = 68.8 MPa, Orifice Dia. = 0.125 mm)

(Speed=71.8 m/min, Feed=12.7 mm/min, Depth=0.89 mm)

Fig. 6 Typical chip shape for (a) flood cooling and (b) high pressure waterjet cooling

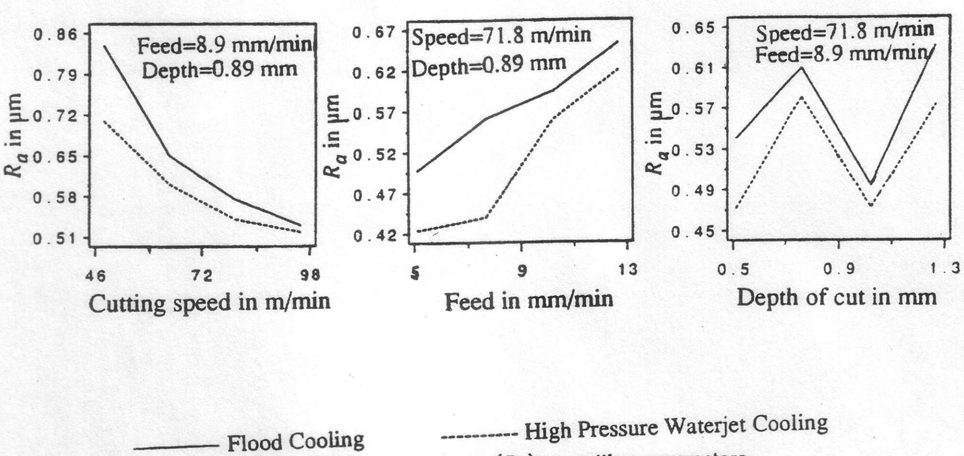

Fig. 5 Surface roughness (R_a) vs. cutting parameters

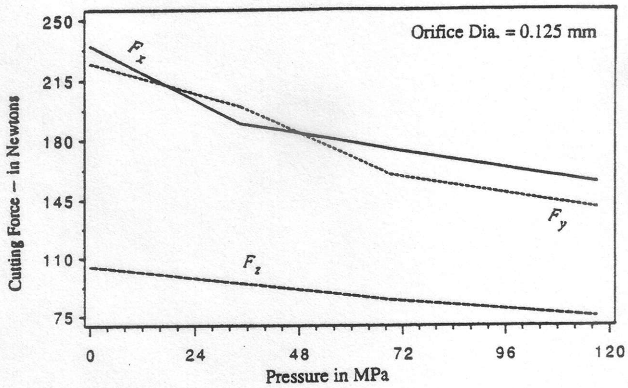

(a) Water Pressure

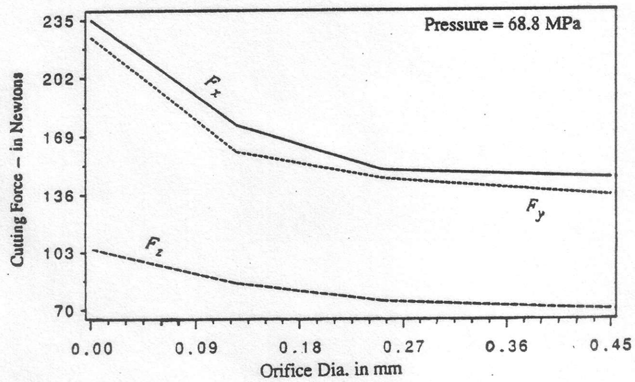

(b) Orifice Diameter

(Speed=71.8 m/min, Feed=8.9 mm/min, Depth=0.89 mm)

Fig. 7 Components of cutting force vs. (*a*) water pressure, and (*b*) orifice diameter

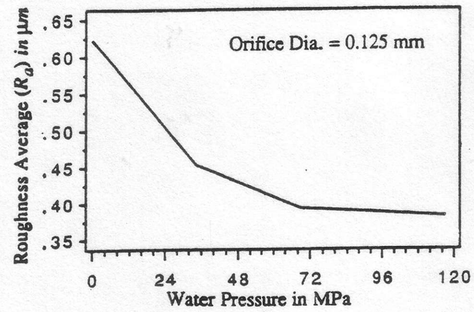

(a) Water Pressure

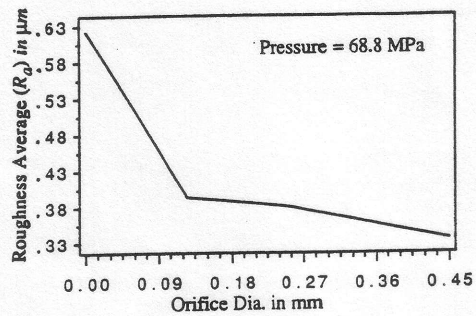

(b) Orifice Diameter

(Speed=71.8 m/min, Feed=8.9 mm/min, Depth=0.89 mm)

Fig. 8 Surface roughness (R_a) vs. (*a*) water pressure, and (*b*) orifice diameter

$$Y_t - \Phi_1 Y_{t-1} - \Phi_2 Y_{t-2} - \ldots - \Phi_n Y_{t-n} = a_t - \Theta_1 a_{t-1} - \Theta_2 a_{t-2} - \ldots - \Theta_{n-1} a_{t-n+1} \quad (1)$$

where, Y_t is the height of the profile at a distance t and $a_t \sim NID(0,\ \sigma_a^2)$. The orders of best fit ARMA models determined using model distance approach [8] were ranging from ARMA (4, 3) to ARMA (2, 1).

The ARMA models are analyzed and the various roots of the models are obtained. The variance decomposition (d_i) of each root gives the relative power of the root. It can be mathematically denoted [11] by,

$$d_i = \frac{g_i g_1}{1-\lambda_i\lambda_1} + \frac{g_i g_2}{1-\lambda_i\lambda_2} + \ldots + \frac{g_i g_n}{1-\lambda_i\lambda_n}, \quad (2)$$

where,

$$g_i = \frac{\lambda_i^{n-1} - \sum_{j=1}^{n-1} \Theta_j \lambda_i^{n-(j+1)}}{\prod_{j=1}^{n} (\lambda_i - \lambda_j)}; \quad i \neq j \quad (3)$$

$(i = 1, 2, \ldots, n)$ and, $\lambda_1, \lambda_2, \ldots, \lambda_n$ are the characteristic roots of the model.

The wavelength decomposition of the roots of the ARMA (n,n−1) model can be derived [11] from the frequency corresponding to each root. Complex roots, say $\lambda_1, \lambda_2 = x \pm iy$ have a damped natural frequency given by,

$$f_d = \frac{1}{2\pi\Delta} \cos^{-1}\left(\frac{x}{\sqrt{x^2+y^2}}\right) \quad (4)$$

where, Δ is the sampling interval.

To distinguish between different real roots causing different concentration of frequencies around zero, a pseudo frequency called break frequency, corresponding to half power point is obtained for each real root.

The break frequency of a real root, say $\lambda_3 = z$, is given by,

$$f_b = \frac{-ln(z)}{2\pi\Delta} \quad (5)$$

The wavelength, W corresponding to each root is given by,

$$W = \frac{\nu}{f} \quad (6)$$

where, ν is the velocity of the stylus and f is the sampling frequency.

The power spectrum density (PSD) of the ARMA models can be defined [12] as,

$$P(f) = \frac{2\sigma_a^2 |1 - \theta_1 e^{-i2\pi f} - \theta_2 e^{-i4\pi f} - \ldots - \theta_{n-1} e^{-i2\pi(n-1)f}|^2}{\gamma_0 |1 - \Phi_1 e^{-i2\pi f} - \Phi_2 e^{-i4\pi f} - \ldots - \Phi_n e^{-i2\pi n f}|^2} \quad (7)$$

where, $0 \le f \le 1/2$ and, $\gamma_0 = \Sigma_{i=1}^{n} d_i$.

Power spectrum density (PSD) of the ARMA models corresponding to the surface profile data, with change in water pressures and orifice diameters are plotted in Figs. 9(*a*) and (*b*), respectively. With increase in water pressure the fre-

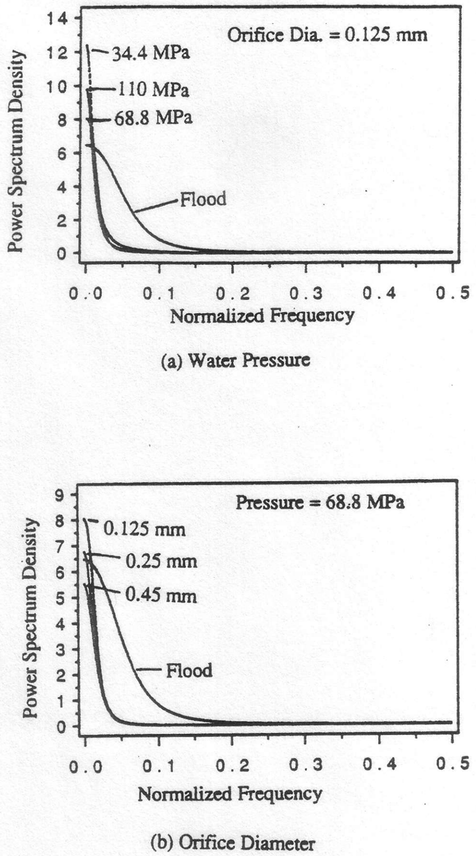

(Speed=71.8 m/min, Feed=8.9 mm/min, Depth=0.89 mm)

Fig. 9 Power spectrum density vs. normalized frequencies for (*a*) different water pressures, and (*b*) orifice diameters

Table 2 Wavelength decomposition—varying water pressures

Sl. No.	Pressure (MPa)	Discrete Roots Real	Discrete Roots Imag.	Power %	Freq. Hz	Wavelength mm
1	0	.6885 .6885	.1478 -.1478	50 50	3.37	.1485
2	34.4	.9392 .5185 -.2393 -.2393	0.000 0.000 -.6748 .6748	105.4 - 6.40 0.50 0.50	.9983 19.58 10.45	.5008 .0255 .0478
3	68.8	.9138 .9138 .0654	.0613 -.0613 0.000	49.5 49.5 1.00	1.066 43.40	.4690 .0155
4	110.08	.9294 .8585 -.5430	0.000 0.000 0.000	157.10 -57.05 -0.05	1.165 2.428 9.719	.4291 .2059 .0514

Table 3 Wavelength decomposition—varying orifice diameters

Sl. No.	Orifice Dia. (mm)	Discrete Roots Real	Discrete Roots Imag.	Power %	Freq. Hz	Wavelength mm
1	0	.6885 .6885	.1478 -.1478	50 50	3.37	.1485
2	0.125	.9138 .9138 .0654	-.0613 .0613 0.000	49.5 49.5 1.00	1.066 43.40	.4690 .0115
3	0.250	.8809 .8809 .1383	.0384 -.0384 .0000	48.7 48.7 2.62	.6933 31.48	.7211 .0159
4	0.450	.8680 .8680 -.5430	.0268 -.0268 0.000	47.5 47.5 4.92	.4912 17.45	1.018 .0286

quency spread reduces, whereas in the case of increase in orifice diameter, the peak of the PSD curve as well as the frequency spread drop gradually. The increase in the orifice diameter tends to smoothen out the surface profile over a broader frequency range. These trends lead to an improvement in surface finish.

The roots and wavelengths obtained for the models representing the surfaces generated for different water pressures are given in Table 2. It can be noted that the surface corresponding to the flood cooling and that produced at a pressure of 68 MPa have complex primary roots whereas the other surfaces have real primary roots. The wavelength corresponding to the flood cooling is approximately equal to the feed per tooth employed in the milling operation. It is interesting to note that the primary wavelength of all the models for different water pressures have a contribution of more than 90 percent on the surface profile. At a pressure of 110 MPa, the secondary wavelength has a considerable negative contribution on the surface profile. This is responsible for better smoothening effect at this pressure.

The dynamic characteristics of the surfaces generated for different orifice diameters are given in Table 3. All the primary roots here are complex roots. The presence of complex roots indicates a better surface finish due to the exponentially decaying dynamic mode. The contribution of the primary roots in the surface profile data is more than 95 percent in all the three cases. Compared to the change in water pressure, orifice diameter change has more influence on the primary wavelength. These trends in the primary wavelength confirm the observation made from the PSD curve.

3.2.4 SEM Photographs of Chips. The SEM photographs of the chips obtained under different water pressures and orifice diameters are shown in Fig. 10. A comparison of the size of the chip produced indicates that the width of the chip produced in the case of flood cooling is much larger than that produced in the case of high pressure waterjet cooling. Further, the width of the chip reduces with increase in the water pressure. This is due to the fact that the chips in the case of flood cooling are subjected to intense heat resulting in more plastic deformation than those produced in the case of high pressure waterjet cooling. The serrations found in the chip indicate the shearing action in the chip formation zone. The serrations of the chip produced in the case of flood cooling are bigger. This is an indication of the high cutting forces in the chip formation zone. By observing the quality of the chip surface in contact with the rake face, in the case of flood cooling, it is found that this surface is rough, indicating the conditions of seizure at the tool-chip interface. The contact surface of the chip with the tool produced in the case of high pressure waterjet cooling is much smoother. Moreover, the reduction in chip width leads to a reduction in tool-chip contact area, consequently reducing frictional forces leading to an improvement in tool life.

3.2.5 Tool Wear. Photographs of carbide inserts used for the high pressure waterjet cooling and flood cooling at two stages of their lives are shown in Fig. 11. A new insert that can be used in conjunction with high pressure waterjet cooling is shown in Fig. 11(*a*). The insert which has been used for 30 min. of operation in conjunction with high pressure waterjet cooling is shown in Fig. 11(*b*) and the corresponding insert used for the case of flood cooling is shown in Fig. 11(*c*). The photographs of the insert after 50 min of operation are shown in Fig. 11(*d*) and Fig. 11(*e*). From these photographs, it can be seen that the width of the flank wear, which is used as a measure of tool life is evidently much larger for the tools used in conjunction with flood cooling than that used for high pressure waterjet cooling.

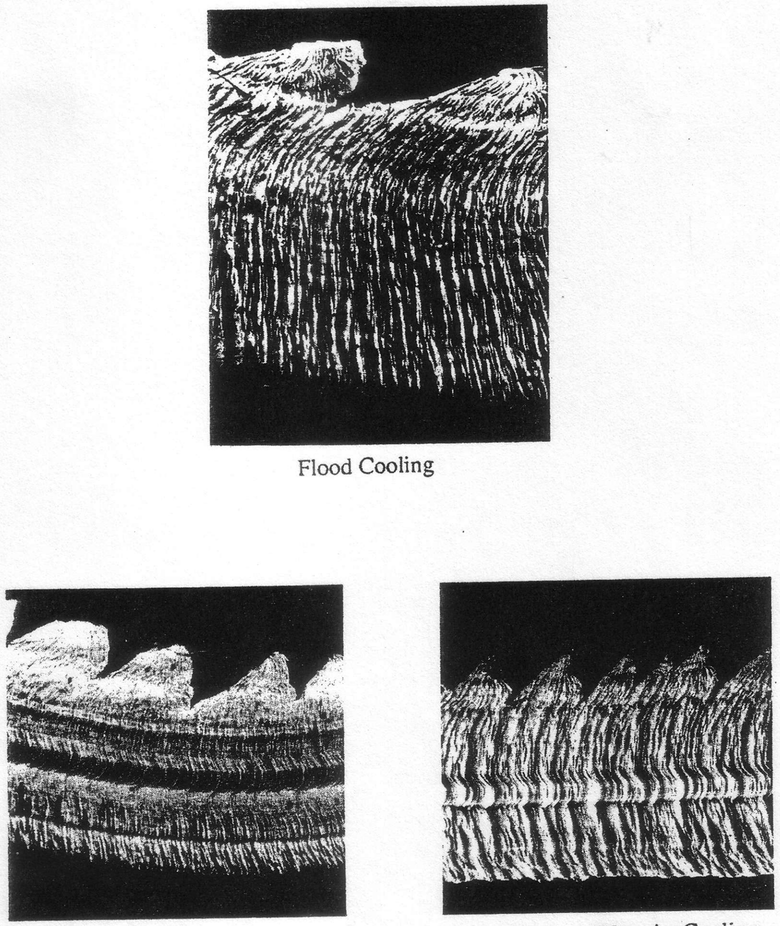

Flood Cooling

High Pressure Waterjet Cooling (Pressure = 68.8 MPa, Orifice Dia. = 0.45 mm)

High Pressure Waterjet Cooling (Pressure = 110 MPa, Orifice Dia. = 0.125 mm)

Fig. 10 SEM photographs of chips (50 ×)

Thus, the insert used for flood cooling gets worn out at a much faster rate than that used for high pressure waterjet cooling.

4 Summary and Conclusions

An apparatus for high pressure waterjet cooling/lubrication at the tool-chip interface in the case of face milling is developed and tested. The system is provided with a specially modified milling cutter which can hold up to five inserts. This apparatus makes use of a high pressure intensifier pump which can pump the fluid at pressures up to 380 MPa. The developed system can be extended to any rotary tool operation although it has been used for face milling in this study. The following conclusions can be deduced based on the investigation conducted:

- There is a considerable reduction in the cutting forces required to remove the material from the workpiece with the application of high pressure waterjet as the coolant/lubricant. Also, the forces continue to reduce steadily with increase in water pressure and orifice diameter.
- The surface finish produced by the high pressure waterjet assisted milling is much better than that produced by flood cooling. In the case of high pressure waterjet cooling, the surface finish improves with increase in water pressure as the high velocity jet is able to penetrate deeper into the regions of tool-chip interface inaccessible in the case of flood cooling. The dynamic characterization of the surface profiles using ARMA modeling further confirms the improvement indicated by the static characteristics.
- Detailed analysis performed on the chip shapes indicates that, the chips produced in the case of high pressure waterjet cooling are comparatively smaller. Lower chip width corresponding to high pressure waterjet cooling leads to a reduction in the tool-chip contact area decreasing the frictional forces at tool-chip interface.
- SEM photographs of the chips indicate that edges of the chip produced in the case of high pressure waterjet cooling are smoother. Further, the serrations found are much smaller than those obtained in the case of flood cooling. This indicates that the frictional conditions existing at the tool-chip interface in high pressure waterjet cooling are not as severe as in the case of flood cooling.
- In this technique, placement of the fluid at the underside of the chip very close to the cutting edge enables to keep the chip away from the rake face minimizing the friction at the tool tip and increasing the rate of heat dissipation from the cutting zone. This leads to reduction in the tool wear and improvement in tool life.
- Finally, the reduction in the cutting forces accompanied by improvement in tool life, surface finish, and chip shape with the use of high pressure waterjet as a coolant/lubricant leads to the possibility of increasing the metal removal rate and thereby improving the cutting efficiency, especially in the case of difficult-to-machine materials.

Acknowledgments

The authors would like to thank the Center for Robotics

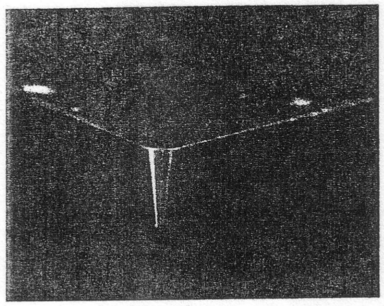

(a) New Insert

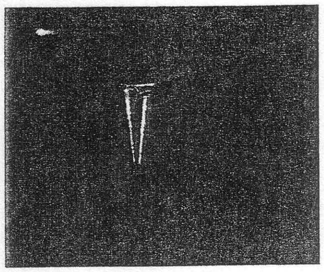

(b) High Pressure Waterjet Cooling

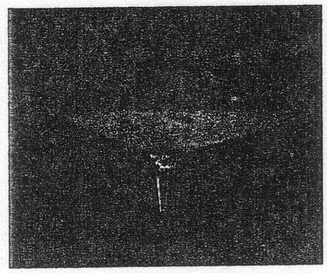

(c) Flood Cooling

Worn Insert after 30 minutes of operation

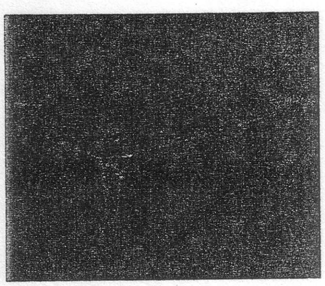

(d) High Pressure Waterjet Cooling
Pressure = 68.8 MPa
Orifice Dia. = 0.125 mm

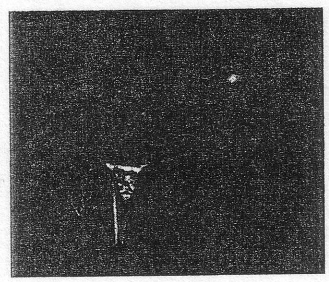

(e) Flood Cooling

Worn Insert after 50 minutes of operation

Fig. 11 Photographs of progressive wear of insert at two stages of tool life

and Manufacturing Systems, University of Kentucky for the financial support in executing this project, Flow International Inc., Kent, Washington, for providing the waterjet cutting system & rotary swivel and Kennametal Inc. for providing the milling machine and tools.

References

1 Pigott, R. J. S., and Colwell, A. T., 1952, "Hi-Jet System for Increasing Tool Life," *SAE Quarterly Transactions*, Vol. 6, No. 3, pp. 547–564.

2 Ramaiyengar, H. S., Salmon, R., and Rice, W. B., 1965, "Some Effects of Cutting Fluids on Chip Formation in Metal Cutting," ASME JOURNAL OF ENGINEERING FOR INDUSTRY, Series B, Vol. 87, pp. 36–38.

3 Sharma, C. S., Rice, W. B., and Salmon, R., 1971, "Some Effects of Injecting Cutting Fluids Directly into the Chip-Tool Interface," ASME JOURNAL OF ENGINEERING FOR INDUSTRY, Vol. 93, pp. 441–444.

4 Mazurkiewicz, M., Kubala, Z., and Chow, J., 1989, "Metal Machining With High-Pressure Water-jet Cooling Assistance—A New Possibility," ASME JOURNAL OF ENGINEERING FOR INDUSTRY, Vol. 111, pp. 7–12.

5 Lindeke, R. R., Schoenig, Jr., F. C., Khan, A. K., and Haddad, J., 1991, "Machining of $\alpha-\beta$ Titanium with Ultra-High Pressure Through the Insert Lubrication/Cooling," *Transactions of NAMRI/SME*, pp. 154–161.

6 Wertheim, R., Rotberg, J., and Ber, A., 1992, "Influence of High-Pressure Flushing through the Rake Face of the Cutting Tool," *Annals of the CIRP*, Vol. 41 No. 1, pp. 101–106.

7 Kovacevic, R., 1994, "Apparatus and Method of High Pressure Waterjet Assisted Cooling/Lubrication in Machining," U.S. Patent No. 5,288,186.

8 Kovacevic, R., and Zhang, Y. M., 1992, "Identification of Surface Characteristics from Large Samples," *Proceedings of the Institute of Mechanical Engineers, Part C, Journal of Mechanical Engineering Science*, Vol. 206, pp. 275–284.

9 Kovacevic, R., Mohan, R., and Cherukuthota, C., 1994, "High Pressure Waterjet as a Coolant/Lubricant in Milling Operation," *ASME PED* Vol. 64, Manufacturing Science and Engineering-1994, pp. 733–748.

10 Kovacevic, R., Cherukuthota, C., and Mohan, R., 1993, "Improving the Surface Quality by High Pressure Waterjet Cooling Assistance," GEOMECHANICS 93, Z. Rakowski, A. A., ed., Balkema/Rotterdam, Brookfield, pp. 305–310.

11 Pandit, S. M., and Shunmugam, M. S., 1992, "Signature of Machine Tool Errors on Surface Texture by DDS," ASME JOURNAL OF ENGINEERING FOR INDUSTRY, Vol. 114, pp. 370–374.

12 Box, G. E. P., and Jenkins, G. M., 1976, *Time Series Analysis, Forecasting and Control*, Holden Day, California.